JBC Papers in Press. Published on January 10, 2002 as Manuscript M110314200

15-Deoxy-$\Delta^{12,14}$-prostaglandin J_2: A prostaglandin D_2 metabolite generated during inflammatory processes

Takahiro Shibata*, Mitsuhiro Kondo*, Toshihiko Osawa*, Noriyuki Shibata†, Makio Kobayashi†, and Koji Uchida*¶

* *Laboratory of Food and Biodynamics, Graduate School of Bioagricultural Sciences, Nagoya University, Nagoya 464-8601, Japan*

† *Department of Pathology, Tokyo Women's Medical University, Tokyo 162-8666, Japan*

Running title: Endogenous production of 15d-PGJ_2

Direct correspondence concerning the manuscript to:

Koji Uchida, Ph.D.

Laboratory of Food and Biodynamics,

Graduate School of Bioagricultural Sciences,

Nagoya University, Nagoya 464-8601, Japan

Tel: 81-52-789-4127, Fax: 81-52-789-5741

E-mail: uchidak@agr.nagoya-u.ac.jp

SUMMARY

Prostaglandin D_2 (PGD_2), a major cyclooxygenase product in a variety of tissues, readily undergoes dehydration to yield the cyclopentenone-type PGs of the J_2-series, such as 15-deoxy-$\Delta^{12,14}$-PGJ_2 (15d-PGJ_2), that have been suggested to exert anti-inflammatory effects *in vivo*. Meanwhile, the mechanism of these effects is not well understood and the natural site and the extent of its production *in vivo* remain unclear. In the present study, we raised a monoclonal antibody specific to 15d-PGJ_2 and determined its production in inflammation-related events. The monoclonal antibody (mAb11G2) was raised against the 15d-PGJ_2-keyhole limpet hemocyanin conjugate and was found to recognize free 15d-PGJ_2 specifically. The presence of 15d-PGJ_2 *in vivo* was immunohistochemically verified in the cytoplasm of most of the foamy macrophages in human atherosclerotic plaques. In addition, the immunostaining of lipopolysaccharide-stimulated RAW264.7 macrophages with mAb11G2 demonstrated an enhanced intracellular accumulation of 15d-PGJ_2, suggesting that the PGD_2 metabolic pathway, generating the anti-inflammatory PGs, is indeed utilized in the cells during inflammation. The activation of macrophages also resulted in the extracellular production of PGD_2, which was associated with a significant increase in the extracellular 15d-PGJ_2 levels, and the extracellular 15d-PGJ_2 production was reproduced by incubating PGD_2 in a cell-free medium and in phosphate-buffered saline. Moreover, using a chiral HPLC method for separation of PGD_2 metabolites, we established a novel metabolic pathway, in which PGD_2 is converted to 15d-PGJ_2 via an albumin-independent mechanism.

The prostaglandins (PGs) are a family of structurally related molecules that are produced by cells in response to a variety of extrinsic stimuli and regulate cellular growth, differentiation and homeostasis (1,2). PGs are derived from fatty acids, primarily arachidonate, which are released from membrane phospholipids by the action of phospholipases. Arachidonate is first converted to an unstable endoperoxide intermediate by cyclooxygenases and subsequently converted to one of several related products, including PGD_2, PGE_2, $PGF_{2\alpha}$, prostacyclin (PGI_2), and thromboxane A_2, through the action of specific PG synthetases. PGD_2, among them, is a major cyclooxygenase (COX) product in a variety of tissues and cells and has marked effects on a number of biological processes, including platelet aggregation, relaxation of vascular and nonvascular smooth muscles and nerve cell functions (3). The PGs are physiologically present in body fluids in picomolar-to-nanomolar concentrations (4); however, arachidonate metabolism is highly increased under several pathological conditions, including hyperthermia, infection and inflammation (5), and local PG concentrations in the micromolar range have been detected at sites of acute inflammation (6). *In vitro*, PGD_2 spontaneously converts into the cyclopentenone PGs of the J series, such as PGJ_2, Δ^{12}-PGJ_2, and 15-deoxy-$\Delta^{12,14}$-PGJ_2 (15d-PGJ_2) (Fig. 1) (7,8). It is not known whether this pathway is utilized in the organism, but it is clear that J_2 prostanoids are synthesized *in vivo*. This is based on the observations that Δ^{12}-PGJ_2 is a natural component of human body fluids (9) and that Δ^{12}-PGJ_2 synthesis is suppressed by treatment with COX inhibitors (9). The natural precursor of PGJ_2 derivatives appears to be PGD_2, because its *in vivo* administration leads to a large increase in Δ^{12}-PGJ_2 (9).

The cyclopentenone PGs have been reported to have their own unique spectrum of biological effects, including inhibition of macrophage-derived cytokine production (10,11) and IκB kinase (12,13), induction of synoviocyte and endothelial cell apoptosis (14), induction of glutathione S-transferase gene expression (15) and intracellular oxidative stress (16), and potentiation of apoptosis in activated macrophages (17). Furthermore, recent studies have reported that they could function as a feedback regulator of the inflammatory response (12,13). However, the mechanism of these effects is not well understood, and the natural site and the extent of their productions *in vivo* remain unclear. Because PGD_2 is the major prostaglandin in most tissues (4), it is likely that the cyclopentenone-type PGD_2

metabolites are produced at a number of sites and may reach functionally significant levels in inflammation and its related disorders. In the present study, we raised a monoclonal antibody specific to 15d-PGJ_2 and determine its endogenous production in human atherosclerotic lesions. Moreover, we investigated the intracellular and extracellular production of 15d-PGJ_2 in the activated RAW264.7 macrophages *in vitro*, and established a novel mechanism of transformation of PGD_2 into the cyclopentenone-type PGJ_2 derivatives, in which PGD_2 is converted to 15d-PGJ_2 via an albumin-independent mechanism.

EXPERIMENTAL PROCEDURES

Material. PGs were purchased from the Cayman Chemical Company (Ann Arbor, MI). Keyhole limpet hemocyanin (KLH) was obtained from Pierce. Horseradish peroxidase-linked anti-rabbit IgG immunoglobulin and ECL (enhanced chemiluminescence) Western blotting detection reagents were obtained from (Amersham Pharmacia Biotech, Buckinghamshire, UK). Lipopolysaccharides (LPS) were obtained from Sigma (St Louis, MO).

Cell culture. Murine RAW264.7 macrophages were kind gifts from Dr. A. Murakami (Kinki University) and Dr. W. Maruyama (National Insititute of Longevity Sciences), respectively. RAW264.7 cells were grown as monolayer cultures in Dulbecco's modified Eagle's medium (DMEM), supplemented with 10% heat-inactivated fetal bovine serum (FBS), penicillin (100 U/ml), streptomycin (100 μg/ml), and 0.2% $NaHCO_3$, at 37 $^{\circ}C$ in an atmosphere of 95% air and 5% CO_2. Cells post-confluency were exposed to LPS (10 μg/ml) in DMEM containing 10% FBS.

Preparation of Anti-15d-PGJ$_2$ Monoclonal Antibody. 15d-PGJ_2 was coupled to KLH by 1-ethyl-3-(dimethylaminopropyl)carbodiimide (EDC) and sulfo-N-hydroxysuccinimide (sulfo-NHS) as described by Grabarek & Gergely (20). Female BALB/c mice were immunized three times with the 15d-PGJ_2-KLH conjugate. Spleen cells from the immunized mice were fused with P3 murine myeloma cells and cultured in HAT (hypoxantine/aminopterin/thymidine) selection medium. Culture supernatants of the hybridoma were screened using ELISA, employing pairs of wells of microtiter plates on which was absorbed 15d-PGJ_2-BSA conjugate as the antigen (0.5 μg of protein/well). After incubation with 100 μl of hybridoma supernatants, and with intervening washes with PBS containing 0.05% Tween 20 (PBS/Tween), the wells were incubated with alkaline phosphatase-conjugated goat antimouse IgG, followed by a substrate solution containing 1 mg/ml *p*-nitrophenyl phosphate. Hybridoma cells corresponding to supernatants that were positive on 15d-PGJ_2-BSA were then cloned by limiting dilution. After repeated screening, two clones were obtained. Among them, clone 11G2 showed the most distinctive recognition

of 15d-PGJ_2-BSA.

Immunoblot Analysis. A gel was transblotted onto a nitrocellulose membrane, incubated with Block Ace (40 mg/ml) for blocking, washed, and treated with anti-COX-2 antibody (Santa Cruz Biotechnology, Santa Cruz, CA). This procedure was followed by the addition of horseradish peroxidase conjugated to a goat anti-mouse IgG $F(ab')_2$ fragment and ECL reagents (Amersham Pharmacia Biotech). The bands were visualized by exposure of the membranes to autoradiography film.

Immunochemical Detection of Intracellular 15d-PGJ_2. Cells were fixed overnight in PBS containing 2% paraformaldehyde and 0.2% picric acid at 4 °C. Membranes were permeabilized by exposing the fixed cells to PBS containing 0.3% Triton X-100. The cells were then incubated sequentially in PBS solutions containing 2% BSA and primary antibody (mAb11G2). The cells were then incubated for 1 h in the presence of FITC-labeled antirabbit IgG (Dako) or Cy™3-labeled goat antimouse IgG (Amersham Pharmacia Biotech), rinsed with PBS containing 0.3% Triton X-100, and covered with anti-fade solution. Images of cellular immunofluorescence were aquired using a confocal laser scanning microscope (FLUOROVIEW, Olympus Optical Co., Ltd, Tokyo) with a 40 x objective (488 nm excitation and 518 nm emmision).

ELISA Analysis of Extracellular PGD_2 and 15d-PGJ_2. Extracellular PGD_2 and 15d-PGJ_2 levels were determined in the culture medium of RAW264.7 macrophages activated with LPS. At the end of the incubation period, the medium was collected and stored at - 80 °C. For determination of PGD_2, a solid phase enzyme immunoassay (Cayman Chemical) was performed as suggested by the manufacturer, and the PGD_2 level was determined using a standard curve and a linear log-logit transformation. For determination of 15d-PGJ_2 in the cell culture medium, the medium (5 ml) was extracted immediately with 3 x 5 ml of ethyl actetate, and the solvent was evaporated under nitrogen. The residue was reconstituted in 200 µl of PBS containing 0.05% Tween 20 (PBS/Tween) and incubated with the antibody (mAb11G2) for 20 h at 4 °C to yield competitor/antibody mixtures containing antibody at 0.2 µg/ml. A 100

μl aliquot of the competitor/antibody mixture was added to each well and incubated for 2 h at 37 °C. After discarding the supernatants and washing three times with PBS/Tween, the second antibody was added, and the enzyme-linked antibody bound to the well was revealed as previously described. The 15d-PGJ_2 levels in the medium were determined using a standard curve and a linear log-logit transformation. For determination of 15d-PGJ_2 upon *in vitro* incubation of PGD_2 in cell-free medium or PBS, an aliquot (200 μl) of the reaction mixtures was directly subjected to the competitive ELISA assay.

Immunochemical Detection of 15d-PGJ2 in Human Atherosclerotic Lesions. Aortic wall samples were obtained at autopsy from five cases of arterial atherosclerosis without diabetes mellitus or any other arterial disorders, performed after their family members granted informed consent. Tissue samples of each case were processed for making frozen materials and used for hematoxylin-eosin stain and immunohistochemical stain. The samples were embedded in OCT compound™ (Sakura Fine Technical Co., Tokyo, Japan), stored at -80 °C, and cut into 6-mm-thick sections by a cryostat. The sections were rehydrated in distilled water, quenched with 3% hydrogen peroxide for 15 min at 4°C, rinsed in PBS, and pretreated with 3% nonimmune serum followed by blocking endogenous avidin/biotin activity using a kit (Vector Laboratories, Burlingame, CA, USA) according to the manufacturer's instructions. The sections were then incubated overnight at 4°C with the primary antibodies. Immunoreaction was visualized by the avidin-biotin-immunoperoxidase complex method using the appropriate Vectastain ABC kit (Vector). Immunostained sections were counterstained with hematoxylin. Sections from which the primary antibodies were omitted served as negative reaction controls.

Separation of PGD_2 Metabolites by Chiral-phase HPLC. Incubation of PGs was carried out in PBS at 37 °C. Samples were withdrawn periodically and extracted immediately with 3 x 0.2 ml of ethyl actetate. The solvent was evaporated under nitrogen and the residue was reconstituted in 50 μl of the chromatographic mobile phase. PG metabolites were separated on a ChiralPak AD-RH column (0.46 x 15 cm) (Daicel Chemical Industries, Ltd., Osaka, Japan) eluted with a linear gradient of

acetonitrile/water/acetic acid (90/10/0.01, by vol.) (solvent A) - acetonitrile (solvent B) (time = 0 – 5 min, 100% A; 60 min, 0% A), at a flow rate of 0.8 ml/min. The elution profiles were monitored by UV absorbance at 200 – 400 nm. Liquid chromatography-mass spectrometry (LC-MS) was measured with a Jasco PlatformII-LC instrument.

RESULTS

Monoclonal Antibody Specific to 15d-PGJ$_2$. 15d-PGJ$_2$ is believed to be physiologically formed through the non-enzymatic conversion of PGD$_2$ but has never been definitively proven to exist *in vivo*. In view of its biological significance, it is critical to provide evidence that 15d-PGJ$_2$ is endogenously produced *in vivo*. To this end, we produced a monoclonal antibody directed to 15d-PGJ$_2$. The antibody was raised against the 15d-PGJ$_2$-KLH conjugate, which was prepared from the reaction of KLH with 15d-PGJ$_2$ in the presence of EDC and sulfo-NHS (Fig. 2A). During the preparation of the monoclonal antibodies, hybridomas were selected on the basis of the ability of their antibodies to bind to the 15d-PGJ$_2$-BSA conjugate. After repeated screening, three clones were obtained. Among them, the antibody produced by the clone 11G2 most strongly recognized the 15d-PGJ$_2$-BSA conjugate but did not recognize the native BSA (Fig. 2B). The antibody was then tested for immunoreactivity with PGs. As shown in Fig. 2C, mAb11G2 recognized 15d-PGJ$_2$ most significantly. Both PGJ$_2$ and Δ^{12}-PGJ$_2$ also served as weak antigens, although their inhibitions were about 50% times lower than 15d-PGJ$_2$. The antibody did not cross-react with other PGs, such as PGA$_2$, PGB$_2$, PGD$_2$, PGE$_2$, PGF$_{2\alpha}$, and PGI$_2$ (data not shown). Taken together, these data indicated that mAb11G2 was directed almost exclusively against the structure of 15d-PGJ$_2$.

Intracellular Accumulation of 15d-PGJ$_2$ in Human Atherosclerotic Lesions. We first examined the *in vivo* presence of 15d-PGJ$_2$ in human atherosclerotic lesions. In broad outline, atherosclerosis is considered to be a form of chronic inflammation. The early stage of atherosclerosis is characterized histopathologically by formation of fatty streaks composed of macrophage-derived foamy cells and exudate-rich extracellular matrix in the intima. The advanced stage of this disease is characterized by increased numbers of foamy macrophages and ulceration and calcification of the fibrously thickened intima. As shown in Fig. 3, intense immunoreactivities for COX-2 (*panel C*) and 15d-PGJ$_2$ (*panel D*) were found to be localized in the cytoplasm of foamy macrophages identified in hematoxylin-eosin-stained (*panel A*) or CD68-immunostained (*panel B*) sections. Aortic wall areas showing atherosclerotic changes

displayed no significant 15-PGJ_2 immunoreactivity. No immunoreaction product deposits were detected in sections with omission of the primary antibodies (data not shown). These observations verified for the first time the intracellular accumulation of 15d-PGJ_2 *in vivo*.

Intracellular Production of 15d-PGJ_2 in the Activated RAW264.7 Macrophages. To examine whether 15d-PGJ_2 is produced in response to inflammatory stimuli *in vitro*, RAW264.7 macrophages were exposed to a pro-inflammatory agent (LPS) and 15d-PGJ_2 produced within the cells was stained with mAb11G2. As shown in Fig. 4A and 4B (*panels a* and *b*), LPS led to a significant induction of COX-2 in RAW264.7 macrophages. Consistent with the COX-2 up-regulation, exposure of the cells to LPS resulted in the appearance of 15d-PGJ_2 immunoreactivity in essentially all cells (Fig. 4B, *panels c* and *d*). An immunofluorescence double-labeling of the activated cells revealed almost identical cellular distribution of COX-2 and 15d-PGJ_2 (Fig. 4C). These results were consistent with the *in vivo* observations that 15d-PGJ_2 was detected intracellularly in the macrophage-derived foam cells in atherosclerotic lesions (Fig. 3). Taken these *in vivo* and *in vitro* data together, it is evident that the production of 15d-PGJ_2, is highly accelerated in the cells during inflammatory processes.

Extracellular Production of 15d-PGJ_2 in the Activated RAW264.7 Macrophages. PGs are synthesized in a broad range of tissue types and serve not only as autocrine but also as paracrine mediators to signal changes within the immediate environment. Hortelano *et al.* (17) have also suggested that 15d-PGJ_2 may contribute to the resolution of inflammation as a paracrine factor. The extracellular production of 15d-PGJ_2 in the activated macrophages was indeed suggested by the observation that the culture medium of macrophages treated with LPS exerted an excitotoxic effect on neurons (data not shown). To examine whether 15d-PGJ_2 is extracellularly produced during inflammation, the levels of 15d-PGJ_2 in the culture medium of the activated macrophages were measured by a competitive ELISA assay. As shown in Fig. 5A, the calibration range (0.1 – 10 nmol) of the standard curve for 15d-PGJ_2 was obtained. In parallel with the COX-2 up-regulation, the extracellular levels of PGD_2 in the LPS-stimulated RAW264.7 macrophages were significantly increased (Fig. 5B). In addition, accompanied by

the production of PGD_2, a significant amount of 15d-PGJ_2 was accumulated in the culture medium (Fig. 5C). The levels of these PGs reached maximums after 12 h of incubation and then decreased thereafter. These data proved that 15d-PGJ_2 was produced extracellularly during inflammatory processes.

Extracellular Conversion of PGD_2 to 15d-PGJ_2 in Cell-Free Medium and in Phosphate-buffered Saline. Because PGD_2 is known to be converted sequentially to the J_2 derivatives of PGs *in vitro* (Fig. 1) (21), it was anticipated that 15d-PGJ_2 could be produced extracellularly in the medium through the metabolism of PGD_2. To examine the extracellular conversion of PGD_2 to 15d-PGJ_2, 1 mM PGD_2 was incubated in the cell-free medium and the formation of 15d-PGJ_2 was examined. As shown in Fig. 6A, 15d-PGJ_2 was detectable by the ELISA assay within 1 h after initiating the incubation. The concentration of 15d-PGJ_2 increased almost linearly from 0 – 8 h and reached a maximum concentration at 24 h. The amount corresponded to the 8% PGD_2 that disappeared during incubation. The maximum levels were maintained for the duration of the experiment.

Serum albumin has been identified as the plasma protein which can catalyze the *in vitro* transformation of PGD_2 into the J_2 derivatives of PGs in aqueous buffer (7). Accordingly, to examine whether serum albumin contained in the medium functioned as a catalyst in the conversion of PGD_2 to 15d-PGJ_2, 1 mM PGD_2 was incubated in PBS containing 10 mg/ml of human serum albumin. As expected, PGD_2 was similarly converted to 15d-PGJ_2 in PBS containing serum albumin (Fig. 6B). However, to our surprise, the conversion was dramatically accelerated in the absence of albumin. These data suggest that serum albumin may be rather inhibitory toward the production of 15d-PGJ_2 from PGD_2.

A Novel PGD_2 Metabolic Pathway. The data (Fig. 6B) contradict the mechanism of PGD_2 metabolism (Fig. 1), in which PGD_2 is sequentially converted to PGJ_2, Δ^{12}-PGJ_2, and 15d-PGJ_2 and the route of conversion leading from PGJ_2 to Δ^{12}-PGJ_2 is catalyzed by serum albumin, therefore suggesting the presence of an albumin-independent mechanism for production of 15d-PGJ_2. To establish a mechanism of transformation of PGD_2 into the cyclopentenone-type PGJ_2 derivatives, we developed a chiral HPLC method for separation of

PGD_2 metabolites and investigated the conventional PGD_2 metabolic pathway in detail. When PGD_2 (1 mM) was incubated in PBS for 24 h, three products (**a**, **b**, and **c**) were mainly detected (Fig. 7A). Over the course of the 24 h period of incubation, no additional abundant products were formed and there were only minor changes in the product pattern (data not shown). The UV spectra of these products were almost indistinguishable. Based on the identical retention time and co-chromatography with authentic PGs, the products **a**, **b**, and **c** were suggested to be PGJ_2, 15d-PGD_2, 15d-PGJ_2, respectively. The identification of the products was finally done by LC-MS analysis of the products, which showed molecular ion peaks at *m/z* 316.4 $(M - H_2O)^+$ (**a**), 334.6 $(M)^+$ (**b**), and 316.9 $(M)^+$ (**c**). It is striking to note that Δ^{12}-PGJ_2, which was reported to be an immediate metabolite of PGJ_2 in the transformation of PGD_2 (21), was not detected in the incubation of PGD_2 alone in PBS. Both PGJ_2 and 15d-PGD_2 were estimated to be generated through dehydration reactions at C-9 and C-15 of PGD_2, respectively, and to be further dehydrated to 15d-PGJ_2. Hence, to identify the direct precursor of 15d-PGJ_2, PGJ_2 and 15d-PGD_2 were individually incubated in PBS at 37 ^{o}C and the products were analyzed by chiral-phase HPLC. As shown in Figs. 7B and 7C, PGJ_2 was stoichiometrically converted to 15d-PGJ_2, whereas no further conversion of 15d-PGD_2 was observed (data not shown). In addition, we were unable to detect Δ^{12}-PGJ_2 upon incubation of PGJ_2 and 15d-PGD_2, suggesting that Δ^{12}-PGJ_2 was not involved in the spontaneous conversion of PGD_2 to the PGJ_2 derivatives. These data indicate that the PGD_2 is primarily converted to three products, including PGJ_2, 15d-PGD_2, and 15d-PGJ_2, among which PGJ_2 is a direct precursor of 15d-PGJ_2.

Serum albumin has been previously identified as the endogenous catalyst of PGD_2 metabolism (7-9). In addition, these workers have identified Δ^{12}-PGJ_2 as the major product in the albumin-catalyzed PGD_2 metabolism. Hence, to characterize the albumin-dependent PGD_2 metabolic pathway, PGD_2 was incubated in PBS containing human serum albumin (10 mg/ml) at 37 ^{o}C, and the products were analyzed by chiral-phase HPLC. As shown in Fig. 8A (*upper chromatogram*), incubation of PGD_2 with human serum albumin yielded, not only the same products (15d-PGD_2, PGJ_2, and 15d-PGJ_2) as those detected in the spontaneous conversion of PGD_2 in albumin-free solution (Fig. 7A), but also a major product which co-chromatographed on HPLC with Δ^{12}-PGJ_2. The LC-MS analysis of the product showed

molecular ion $(M)^+$ peak at *m/z* 334.8, which coincided with the theoretical molecular weight of Δ^{12}-PGJ_2. Thus, the product was determined to be Δ^{12}-PGJ_2. It was observed that PGJ_2 was converted to both 15d-PGJ_2 and Δ^{12}-PGJ_2 in the presence of human serum albumin (Fig. 8A, *middle*). Moreover, no further conversion of Δ^{12}-PGJ_2 was observed (Fig. 8A, *bottom*), indicating that Δ^{12}-PGJ_2 represents one of the terminal product of PGD_2 metabolism. Isomerization of PGJ_2 to Δ^{12}-PGJ_2 was dependent on the incubation time and the concentration of human serum albumin: when human serum albumin was present in excess, PGJ_2 was almost stoichiometrically converted to Δ^{12}-PGJ_2 (Fig. 8B). Boiling of serum albumin markedly decreased the formation of Δ^{12}-PGJ_2 from PGJ_2 but did not affect the formation of 15d-PGJ_2 (Fig. 8C), suggesting that Δ^{12}-PGJ_2 is formed by the enzymatic action of albumin while 15d-PGJ_2 is a nonenzymatically formed product.

Taken together, these data suggest that PGD_2 is sequentially converted to PGJ_2 and 15d-PGJ_2 in an albumin-independent manner and serum albumin is involved only in the process leading from PGJ_2 to Δ^{12}-PGJ_2 (Fig. 9).

DISCUSSION

Immunochemical detection is a powerful tool that can be used to evaluate the presence of a desired target and its subcellular localization. The major advantages of this technique over other biochemical approaches are the evaluation of small numbers of cells or archival tissues that may otherwise not be subject to analysis. In this study, we obtained a murine monoclonal antibody, mAb11G2, that clearly distinguished the 15d-PGJ_2-protein conjugate from the native protein. Characterization of the antibody revealed that the monoclonal antibody was directed almost exclusively against free 15d-PGJ_2 (Fig. 2). It was expected that mAb11G2 would be useful in assessing the endogenous production of 15d-PGJ_2 in response to inflammatory stimuli. *In vivo* detection of 15d-PGJ_2 using mAb11G2 was first attempted in the tissue samples from the patients with atherosclerosis. Atherosclerosis is considered to be a form of chronic inflammation resulting from interaction between modified lipoproteins, monocyte-derived macrophages, T cells, and the normal cellular elements of the arterial wall. This inflammatory process can ultimately lead to the development of complex lesions, or plaques, that protrude into the arterial lumen. In the present study, we confirmed that atheromatous lesions indeed contained high levels of COX-2, colocalizing mainly with foamy macrophages (Fig. 3*C*). In addition, 15d-PGJ_2 was also found to localize predominantly with the lesional macrophages (Fig. 3*D*). These observations raise the possibility that 15d-PGJ_2 may play a role in the pathogenesis of inflammation-related disorders, such as atherosclerosis.

Activation of the host immune system by Gram-negative bacteria can be reproduced *in vitro* by incubation of cells with LPS and pro-inflammatory cytokines. Macrophages participate actively in the onset of inflammation and immune system activation by releasing cytokines that amplify the initial inflammatory stimulation, bioactive lipids (*e.g.*, PGs and leukotrienes), reactive oxygen species and reactive nitrogen species that exert cytotoxic effects against pathogens and tumor cells (22-25). As result of activation, macrophages express pro-inflammatory enzymes, such as COX-2, nitric oxide synthase-2, and matrix metalloproteinases (25) and produce an array of prostanoids, including PGE_2 and thromboxane A_2 (26), considered the more atherogenic eicosanoids. In the present study, we

provided evidence that the production of 15d-PGJ_2 was augmented in the activated RAW264.7 macrophages with LPS *in vitro* (Fig. 4). These data coincided with the observation that the 15d-PGJ_2 synthesis was predominantly enhanced in the macrophage-derived foam cells *in vivo* (Fig. 3). It is suggested that the enhanced production of 15d-PGJ_2 in the activated macrophages may represent an inflammatory response, which contributes to negative regulation of inflammation. Recent studies have shown that 15d-PGJ_2 is a high-affinity ligand for peroxisome proliferator-activated receptor γ (PPARγ) (27,28). 15d-PGJ_2 represses several genes in activated macrophages, including the inducible nitric oxide synthase and tumor necrosis factor α genes, and this repression is suggested to be at least partly dependent on PPARγ expression (10,11,29). The anti-inflammatory effect of 15d-PGJ_2 has also been deduced from models of carrageenin-induced inflammation in which a two-phase PG release has been described after expression of COX-2: PGE_2 synthesis predominates during the early inflammatory step, whereas 15d-PGJ_2 substitutes PGE_2 formation at the end of the process, coincident with the accumulation of macrophages (30,31). Therefore, the physiopathological relevance of the enhanced synthesis of 15d-PGJ_2 in activated macrophages may represent a mechanism in which 15d-PGJ_2 functions as a feedback regulator of the inflammatory reponses (31).

On the other hand, recent studies have shown that 15d-PGJ_2 directly inhibits the NF-κB-dependent gene expression through covalent modifications of critical cysteine residues in IκB kinase and the DNA-binding domains of NF-κB subunits (12,13), leading to the PPARγ-independent resolution of inflammation. Several previous observations have also indicated that PGD_2 and its J-ring metabolites might exert effects through interactions with intracellular proteins: (*i*) Narumiya *et al.* (32) have shown that radiolabeled Δ^{12}-PGJ_2 is actively incorporated into cells and transferred to the nucleus, where it is associated with proteins; (*ii*) some PGs, including PGD_2, PGJ_2, and Δ^{12}-PGJ_2, have been shown to bind with high affinity to liver fatty acid-binding protein and intracellular protein involved in the uptake, intracellular transport, and metabolism of free fatty acids and their acyl-CoA esters (33). The A and J series of PGs are characterized by the presence of a cyclopentenone ring system that contains an electrophilic carbon that can react covalently by means of the Michael addition reaction with nucleophiles, such as the free sulfhydryls of glutathione and cysteine residues in cellular

proteins (21,34,35). This reactive center is not present in the synthetic PPARγ ligands and has been proposed to account for some of the receptor-independent biological actions of PGJ_2, its metabolites, and the related cyclopentenone PGs, such as PGA_1 and PGA_2 (34,35).

Cyclopentenone PGs have also been viewed as important factors in the resolution of the inflammatory process through the potentiation of cell death. The recent study shows that 15d-PGJ_2 plays a role in the resolution of inflammation by inducing apoptosis of activated macrophages (17). In addition, the observations that the J_2 series of the PGs represent the most potent inducers of intracellular oxidative stress and that the production of reactive oxygen species in the cells is closely associated with the excitotoxic effect of the PGs (16) raises the possibility that the production of cyclopentenone PGs during inflammation may be causally involved in the pathophysiological effects associated with degenerative cell loss. Indeed, we have detected the 15d-PGJ_2 immunoreactivity in the motor neurons in spinal cords from sporadic amyotrophic lateral sclerosis patients (Shibata, T., Kondo, M., Shibata, N., Kobayashi, M., Osawa, T., & Uchida, K., unpublished observation). Future studies are needed to determine whether and how enhanced 15d-PGJ_2 production functionally affects cell death during inflammatory processes and the net effect *in vivo* of the interplay between the anti- and pro-inflammatory products of COX in human diseases.

The accumulation of significant amounts of 15d-PGJ_2 was observed in the cell culture medium of activated macrophages (Fig. 5), suggesting the involvement of mechanisms by which (*i*) 15d-PGJ_2 is produced intracellularly followed by excretion to the medium and/or (*ii*) 15d-PGJ_2 is produced in the medium through the nonenzymatic conversion of PGD_2. The latter possibility was attested to by the observations that the *in vitro* incubation of PGD_2 in the cell-free medium resulted in increased 15d-PGJ_2 immunoreactivity (Fig. 6A). The data suggested that 15d-PGJ_2 could be produced extracellularly *via* nonenzymatic conversion of PGD_2 and may function as an autocrine and paracrine factor during inflammatory processes (Fig. 10). The *in vitro* synthesis of 15d-PGJ_2 was first reported by Fitzpatrick and Wynalda (7). These authors have shown that human serum albumin catalyzes the *in vitro* transformation of PGD_2 into three dehydration products, such as Δ^{12}-PGJ_2, 15d-PGD_2, and 15d-PGJ_2. The present study also confirmed the production of 15d-PGJ_2 upon incubation of PGD_2 with serum albumin (Fig. 6A). However, it is striking to note that the *in vitro* conversion of PGD_2

to 15d-PGJ_2 was further accelerated in the absence of serum albumin (Fig. 6B). In other words, serum albumin was highly inhibitory toward the production of 15d-PGJ_2 (Fig. 9). The data contradict the mechanism of formation of PGJ_2 derivatives (Fig. 1), in which PGD_2 is sequentially converted to PGJ_2, Δ^{12}-PGJ_2, and 15d-PGJ_2 and the route of conversion leading from PGJ_2 to Δ^{12}-PGJ_2 is catalyzed by serum albumin. To reinvestigate the PGD_2 biometabolic pathway. we developed a chiral-phase HPLC method for separation of PGD_2 metabolites and characterized the PGD_2 metatbolic pathway in detail. We detected four products that originate from transformation of PGD_2, namely: 15d-PGD_2, PGJ_2, Δ^{12}-PGJ_2, and 15d-PGJ_2. PGD_2 may be initially converted to the dehydration products, PGJ_2 and 15d-PGD_2 (Fig. 9). It is suggested that the ketone group of PGD_2 at C_{11} facilitates the β-elimination of hydroxyl group at C_9 to form PGJ_2, whereas a proton at C_{12} that is simultaneously allylic and α to the C_{11} carbonyl facilitates isomerization of the β,γ-unsaturated enone to a more stable α,β-unsaturated enone followed by dehydration to form 15d-PGD_2. These initial dehydration reactions proceed independently of serum albumin. The observations that (*i*) incubation of PGD_2 without serum albumin generated 15d-PGD_2, PGJ_2, and 15d-PGJ_2, but not Δ^{12}-PGJ_2, (Fig. 7A) and (*ii*) PGJ_2 was stoichiometrically converted to 15d-PGJ_2 without generating Δ^{12}-PGJ_2 (Fig. 7B) indicate that PGJ_2 is directly converted to 15d-PGJ_2. Therefore, it appears that PGD_2 is sequentially converted to PGJ_2 and 15d-PGJ_2 in an albumin-independent manner (Fig. 9). It is likely that formation of an α,β-unsaturated ketone within the cyclopentenone ring facilitate Δ^{12} isomerization followed by dehydration of the C_{15} hydroxyl. In the presence of serum albumin, Δ^{12}-PGJ_2, in addition to 15d-PGD_2, PGJ_2, and 15d-PGJ_2, was newly detected (Fig. 8A). Serum albumin catalyzed the stoichiometric conversion of PGJ_2 to Δ^{12}-PGJ_2 (Fig. 8A), which was significantly inhibited by the addition of linoleic acid, a ligand of albumin (data not shown). In addition, boiling of serum albumin markedly decreased the formation of Δ^{12}-PGJ_2 from PGJ_2 but did not affect the formation of 15d-PGJ_2 (Fig. 8C), suggesting that Δ^{12}-PGJ_2 is formed by the enzymatic action of albumin. These data suggest that serum albumin is involved only in the process leading from PGJ_2 to Δ^{12}-PGJ_2 (Fig. 9).

In summary, we obtained a new murine monoclonal antibody, mAb11G2, that clearly distinguished 15d-PGJ_2 from other PGs. Using this antibody, the *in vivo* presence of 15d-PGJ_2 was first demonstrated in the cytoplasm of most of the foamy or spindle macrophages in

human atherosclerotic plaques. In addition, the intracellular production of 15d-PGJ_2 was observed in the activated RAW264.7 macrophages with LPS. We also observed the accumulation of 15d-PGJ_2 in the culture medium of activated macrophages and the spontaneous conversion of PGD_2 to 15d-PGJ_2 in the cell-free medium. Thus, 15d-PGJ_2 was produced not only intracellularly but also extracellularly *via* nonenzymatic conversion of PGD_2, suggesting that 15d-PGJ_2 could function as both autorine and paracrine factors. 15d-PGJ_2 accumulated in activated macrophages has been suggested to be involved in the regulation of inflammatory responses. The present study may stimulate further efforts to understand mechanisms regulating the production and biological roles of 15d-PGJ_2 *in vivo*.

Acknowledgments — We thank Dr. A. Murakami (Kinki University) for the cell lines.

REFERENCES

1. Smith, W.L. (1989) *Biochem. J.* **259**, 315-324.
2. Smith, W.L. (1992) *Am. J. Physiol.* **263**, F181-191.
3. Giles H. & Leff, P. (1988) *Prostaglandins* **35**, 277-300.
4. Fukushima, M. (1990) *Eicosanoids* **3**, 189-199.
5. Herschman, H.R., (1997) *Adv. Exp. Med. Biol.* **407**, 61-66.
6. Offenbacher, S., Odle, B.M., & Van Dyke, T.E. (1986) *J. Periodontal Res.* **21**, 101-112.
7. Fitzpatrick, F.A. & Wynalda, M.A. (1983) *J. Biol. Chem*. **258**, 11713-11718.
8. Kikawa, Y., Narumiya, S., Fukushima, M., Wakatsuka, H. & Hayaishi, O. (1984) *Proc. Natl. Acad. U.S.A.* **81**, 1317-1321.
9. Hirata, Y., Hayashi, H., Ito, S., Kikawa, Y., Ishibashi, M., Sudo, M., Miyazaki, H., Fukushima, M., Narumiya, S., & Hayashi, O. (1988) *J. Biol. Chem.* **263**, 16619-16625.
10. Ricote, M., Li, A.C., Willson, T.M., Kelly, C.J., & Glass, C.K. (1998) *Nature* **391**, 79-82.
11. Jiang, C., Ting, A.T., & Seed, B. (1998) *Nature* **391**, 82-86.
12. Rossi, A., Kapahi, P., Natoli, G., Takahashi, T., Chen, Y., Karin, M., & Santoro, M.G. (2000) *Nature* **403**, 103-108.
13. Straus, D., Pascual, G., Li, M., Welch, J.S., Ricote, M., Hsiang, C.-H., Sengchanthalangsy, L.L., Ghosh, G., & Glass, C.K. (2000) *Proc. Natl. Acad. Sci. U.S.A.* **97**, 84844-4849.
14. Bishop-Bailey, D. & Hla, T. (1998) *J. Biol. Chem*. **274**,17042-17048.
15. Kawamoto, Y., Nakamura, Y., Naito, Y., Torii, Y., Kumagai, T., Osawa, T., Ohigashi, H., Satoh, K., Imagawa, M., & Uchida, K. (2000) *J. Biol. Chem*. **275**, 11291-11299.
16. Kondo, M., Oya-Ito, T., Kumagai, T., Osawa, T., & Uchida, K. (2001) *J. Biol. Chem.* **276**, 12076-12083.
17. Hortelano, S., Castrillo, A., Alvarez, A.M., & Bosca, L. (2000) *J. Immunol.* **165**, 6525-6531.
18. Narayanan, P.K., Goodwin, E.H., & Lehnert, B.E. (1997) *Cancer Res.* **57**, 3963-3971.
19. Rothe, G. & Valet, G. (1990) *J. Leukoc. Biol*. **47**, 440-448.
20. Grabarek, Z. & and Gergely, J. (1990) *Anal. Biochem*. **185**, 131-135.
21. Fukushima, M. (1992) *Prostaglandins Leukot. Essent. Fatty Acids* **47**, 1-12.

22. MacMicking, J., Xie, Q.W., & Nathan, C. (1997) *Ann. Rev. Immunol.* 15, 323-350.

23. Molloy, A., Laochumroonvorapong, P., & Kaplan, G. (1994) *J. Exp. Med*. **180**, 1499-1509.

24. Thompson, C.B. (1995) *Science* **267**, 1456-1462.

25. Bogdan, C., Rollinghoff, M., & Diefenbach, A. (2000) *Curr. Opin. Immunol.* **12**, 64.

26. Fu, J.Y., Masferre, J.L., Seibert, K., Raz, A., & Needleman, P. (1990) *J. Biol. Chem.* **265**, 16737-16740.

27. Forman, B.M., Tontonoz, P., Chen, J., Brun, R.P., Spiegelman, B.M., & Evans, R.M. (1995) *Cell* **83**, 803-812.

28. Kliewer, S.A., Lenhard, J.M., Willson, T. M., Patel, I., Morris, D.C., & Lehmann, J.M. (1995) *Cell* **83**, 813-819.

29. Marx, N., Scheonbeck, U., Lazar, M.A., Libby, P. & Plutzky, J. (1998) *Circ. Res.* **83**, 1097-1103.

30. Fournier, T., Fadok, V., & Henson, P.M. (1997) *J. Biol. Chem*. **272**, 31065 –31072.

31. Gilroy, D.W., Colville-Nash, P.R., Willis, D., Chivers, J., Paul-Clark, M.J., & Willoughby, D.A. (1999) *Nat. Med.* **5**, 698-701.

32. Narumiya, S., Ohno, K., Fukushima, M., & Fujiwara, M. (1987) *J. Pharmacol. Exp. Therap.* **242**, 306-311.

33. Khan, S.H. & Sorof, S. (1990) *Proc. Natl. Acad. Sci. U.S.A.* **87**, 9401-9405.

34. Rossi, A., Elia, G., & Santoro, M.G. (1996) *J. Biol. Chem*. **271**, 32192-32196.

35. Bui, T. & Straus, D.S. (1998) *Biochim. Biophys. Acta* **1397**, 31-42.

FOOTNOTE

This work was supported in part by Program for Promotion of Basic Research Activities for Innovative Biosciences (PROBRAIN).

¶ To whom correspondence should be addressed: Koji Uchida, Laboratory of Food and Biodynamics, Graduate School of Bioagricultural Sciences, Nagoya University, Nagoya 464-8601, Japan. Fax: 81-52-789-5741. E-mail: uchidak@agr.nagoya-u.ac.jp

Abbreviations**:** PGs, prostaglandins; 15d-PGJ_2, 15-deoxy-$\Delta^{12,14}$-PGJ_2; PGD_2, prostaglandin D_2; KLH, keyhole limpet hemocyanin; EDC, 1-ethyl-3-(dimethylaminopropyl)carbodiimide; sulfo-NHS, sulfo-N-hydroxysuccinimide; DCFH-DA, 2',7'- dichlorofluorescein-diacetate;LPS. lipopolysaccharides; COX-2, cyclooxygense-2; ROS, reactive oxygen species; ELISA, enzyme-linked immunosorbent assay; PPARγ, peroxisome proliferator-activated receptor γ.

LEGENDS TO FIGURES

Fig. 1. The PGD_2 metabolic pathway.

Fig. 2. Preparation of a monoclonal antibody against 15d-PGJ_2. (*A*) Preparation of antigen (15d-PGJ_2-KLH conjugate). (*B*) Immunoreactivity of mAb11G2 to the 15d-PGJ_2-BSA conjugate. *Symbols*: ○, BSA; ●, 15d-PGJ_2-BSA conjugate. (*C*) Immunoreactivity of mAb11G2 to PGs. Affinity of antibody was determined by a competitive ELISA. Competitors: ○, arachidonate; ●, 15d-PGJ_2; ■, Δ^{12}-PGJ_2; △, PGD_2; ▲, 15d-PGD_2; ◆, PGJ_2.

Fig. 3. Immunohistochemical detection of 15d-PGJ_2 in human atherosclerotic aorta. Arterial tissue specimens were stained with hematoxylin-eosin (*A*) and immunostained with anti-CD68 antibody (*B*), anti-COX-2 antibody (*C*), and mAb11G2 (*D*). *A*-*C*, x40.

Fig. 4. Intracellular production of 15d-PGJ_2 in the activated RAW264.7 macrophages. (*A*) Immunoblot analysis of COX-2 in RAW264.7 macrophages exposed to LPS. (*B*) Immunocytochemical detection of COX-2 (*panels a* and *b*) and 15d-PGJ_2 (*panels c* and *d*) in the activated RAW264.7 macrophages. The cells were exposed to 10 μg/ml LPS for 24 h at 37 °C. Fluorescein isothiocyanate fluorescence (COX-2, *green*) is shown in the *upper panels* (*a* and *b*); Cy™3 fluorescence (15d-PGJ_2, *red*) is shown in the *lower panels* (*c* and *d*). (*C*) An immunofluorescence double-labeling of activated RAW264.7 macrophages. The cells were exposed to 10 μg/ml LPS for 24 h at 37 °C.

Fig. 5. Extracellular production of PGD_2 and 15d-PGJ_2 in the activated RAW264.7 macrophages. RAW264.7 macrophages were incubated with 10 μg/ml LPS and the amounts of PGD_2 and 15d-PGJ_2 released into the medium were measured. (*A*) A standard curve for 15d-PGJ_2 in a competitive ELISA. Competitor: 15d-PGJ_2. (*B*) Extracellular production of PGD_2. (*C*) Extracellular production of 15d-PGJ_2. In *panels B* and *C*, the data represent means ± SD of triplicate determinations.

Fig. 6. Conversion of PGD_2 to 15d-PGJ_2 in cell-free medium and in phosphate-buffered saline. (*A*) Conversion of PGD_2 to 15d-PGJ_2 in cell-free medium. PGD_2 (1 mM) was incubated in the cell-free DMEM, supplemented with 10% heat-inactivated fetal bovine serum (FBS), penicillin (100 U/ml), streptomycin (100 μg/ml), and 0.2% $NaHCO_3$, at 37 °C. (*B*) Conversion of PGD_2 to 15d-PGJ_2 in the presence and absence of human serum albumin. PGD_2 (1 mM) in PBS was incubated in the presence (○) and absence (●) of serum albumin (10 mg/ml) at 37 °C. The 15d-PGJ_2 levels in the reaction mixtures were determined by a competitive ELISA assay. The data represent means ± SD of triplicate determinations.

Fig. 7. Chiral-phase HPLC analysis of PGD_2 metabolites. PGD_2 and its metabolites were separated on a ChiralPak AD-RH column (0.46 x 15 cm) eluted with a linear gradient of acetonitrile/water/acetic acid (90/10/0.01, by vol.) (solvent A) - acetonitrile (solvent B) (time = 0 – 5 min, 100% A; 60 min, 0% A), at a flow rate of 0.8 ml/min. The elution profiles were monitored by UV absorbance at 200 – 400 nm. (*A*) HPLC profile of PGD_2 metabolites. Incubation of PGD_2 (1 mM) was carried out in PBS for 24 h at 37 °C. (*B*) HPLC profile of PGJ_2 metabolites. Incubation of PGJ_2 (1 mM) was carried out in PBS for 24 h at 37 °C. (*C*) Stoichiometry of consumption of PGJ_2 (○) and concomitant formation of 15d-PGJ_2 (●).

Fig. 8. Conversion of PGD_2 to the PGJ_2 derivatives in the presence of human serum albumin. PGD_2 and its metabolites were separated on a ChiralPak AD-RH column (0.46 x 15 cm) eluted with a linear gradient of acetonitrile/water/acetic acid (90/10/0.01, by vol.) (solvent A) - acetonitrile (solvent B) (time = 0 – 5 min, 100% A; 60 min, 0% A), at a flow rate of 0.8 ml/min. The elution profiles were monitored by UV absorbance at 200 – 400 nm. (*A*) HPLC profile of 1 mM PGD_2 (*top*), PGJ_2 (*middle*), and Δ^{12}-PGJ_2 (*bottom*), incubated in PBS containing 10 mg/ml human serum albumin for 24 h at 37 °C. (*B*) Stoichiometry of consumption of PGJ_2 (○) and concomitant formation of Δ^{12}-PGJ_2 (●) and 15d-PGJ_2 (▲). (*C*) HPLC profile of 1 mM PGJ_2 incubated in PBS containing 10 mg/ml native (*lower*) or boiled (*upper*) human serum albumin for 24 h at 37 °C. Human serum albumin was boiled for 5 min prior to incubation.

Fig. 9. A revised pathway of PGD_2 metabolism.

Fig. 10. Model for mechanisms by which PGD_2 is intracellularly and extracellularly metabolized to 15d-PGJ_2.

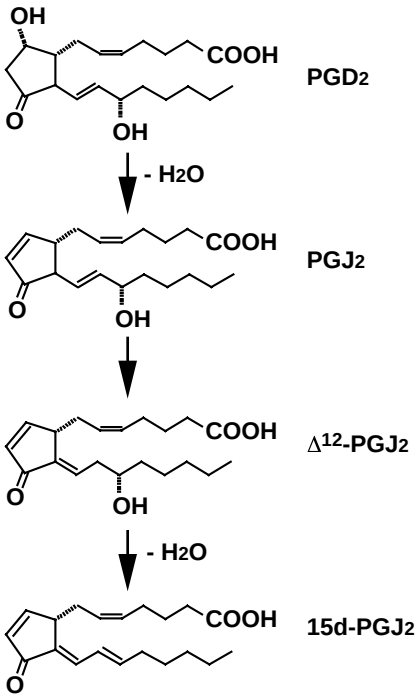

Fig. 1

Shibata et al.

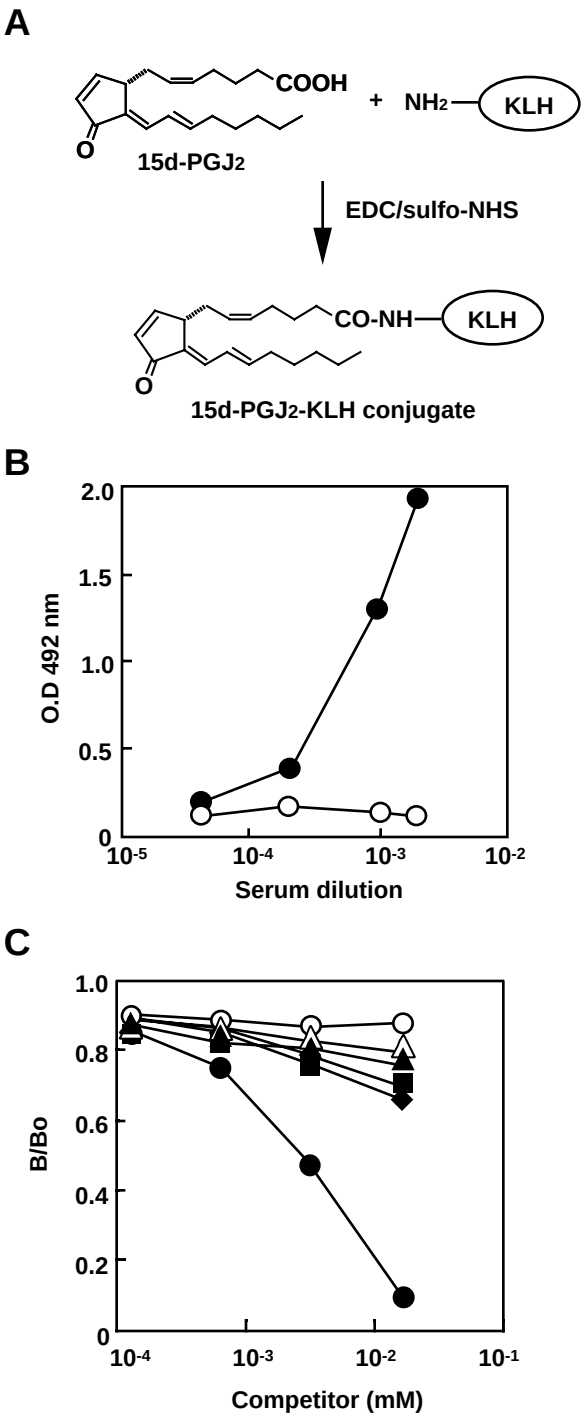

Fig. 2

Shibata et al.

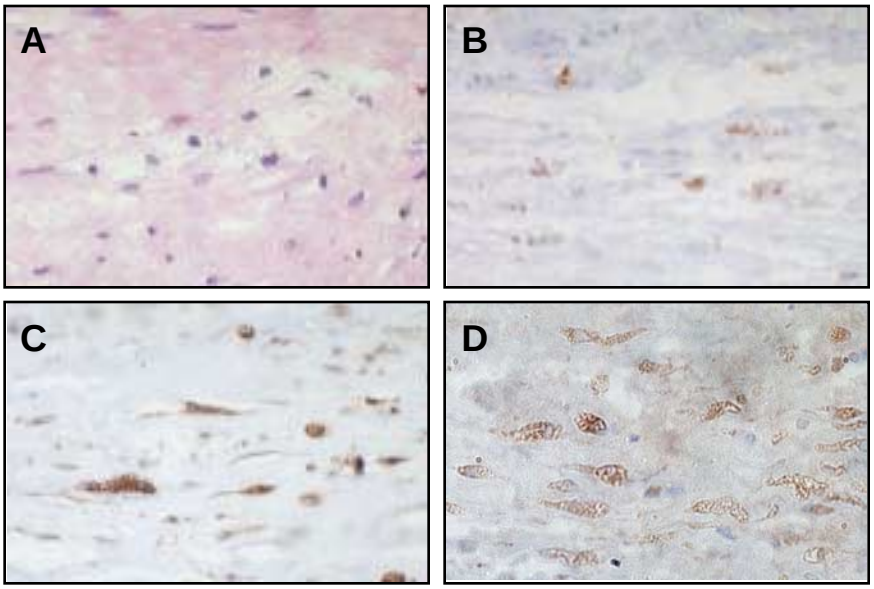

Fig. 3

Shibata et al.

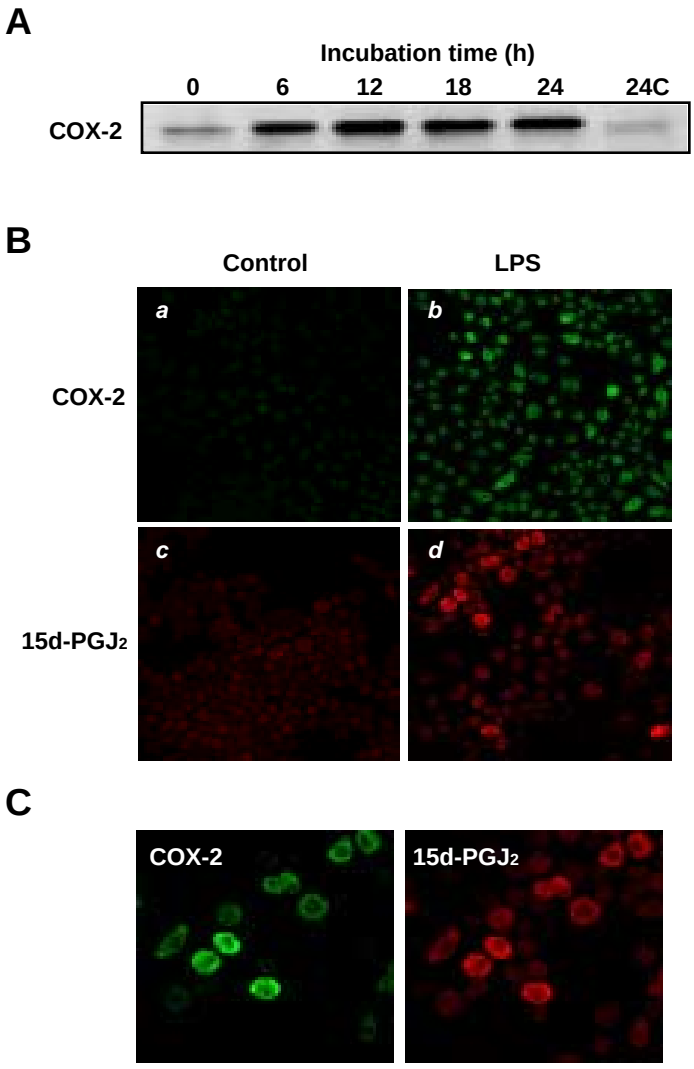

Fig. 4

Shibata et al.

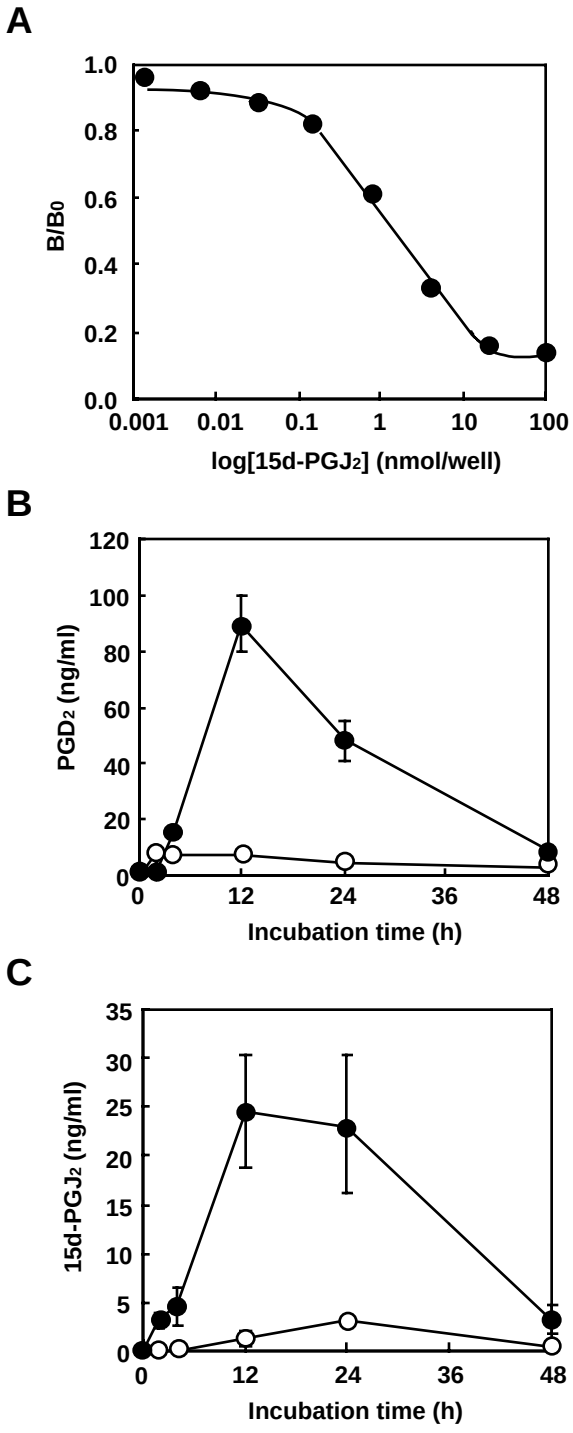

Fig. 5

Shibata et al.

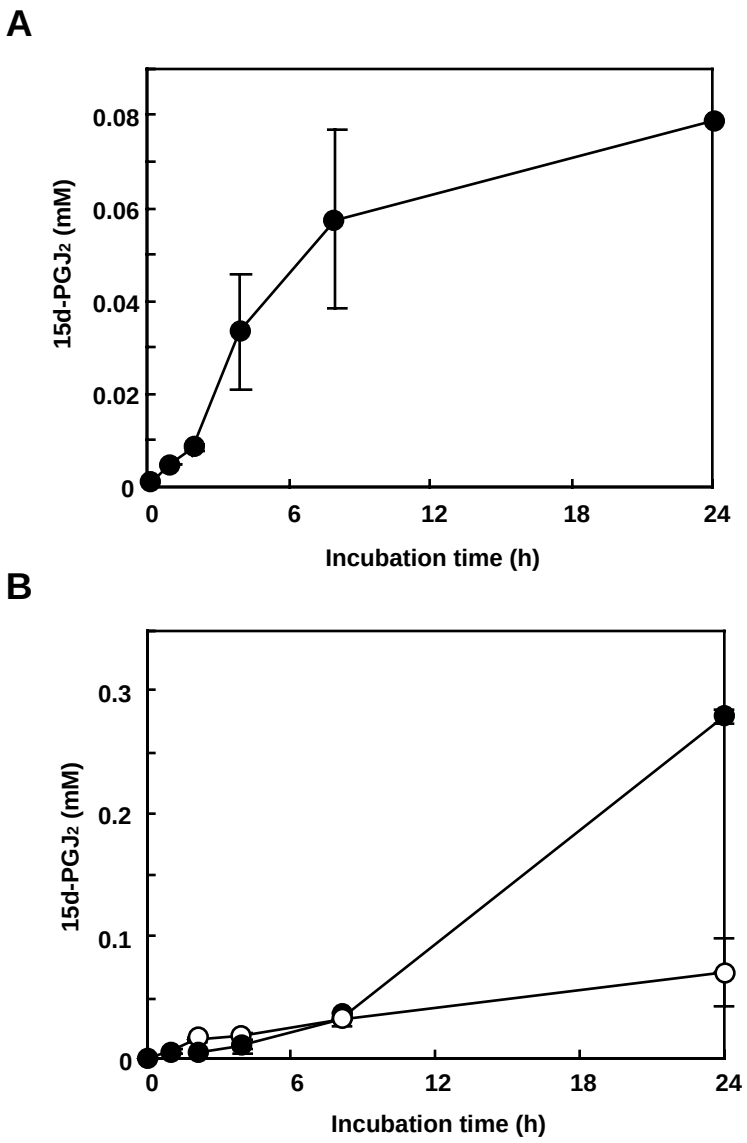

Fig. 6

Shibata et al.

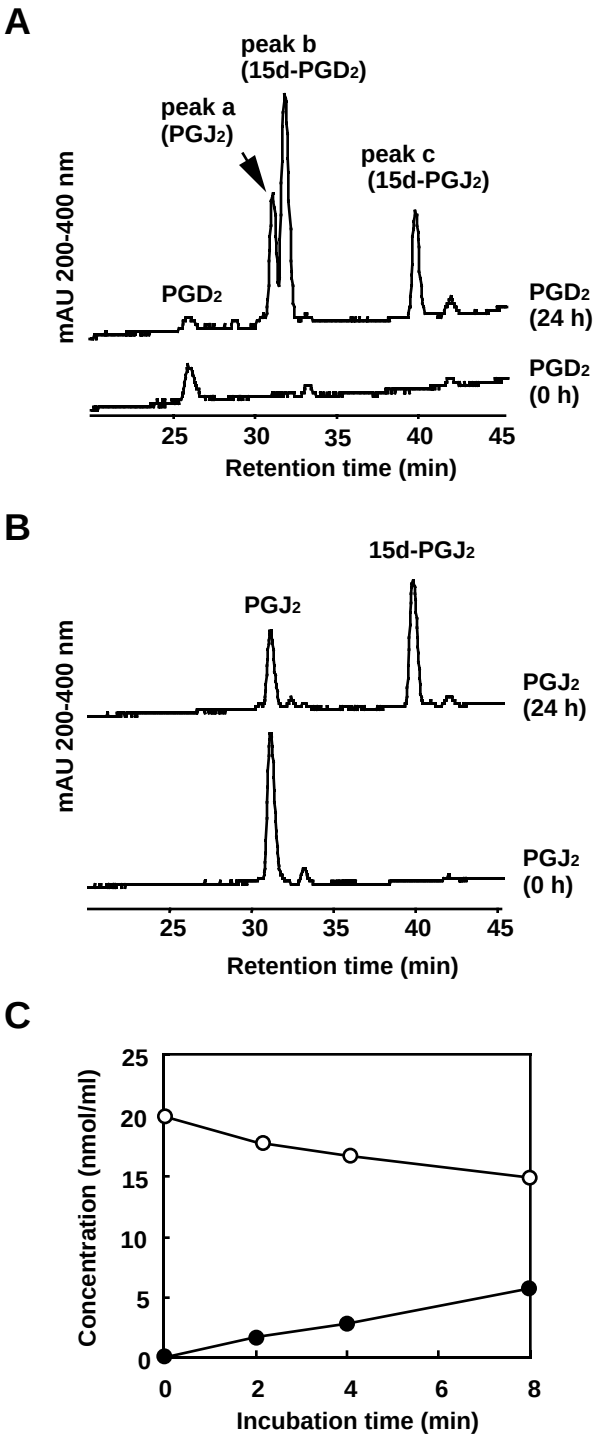

Fig. 7

Shibata et al.

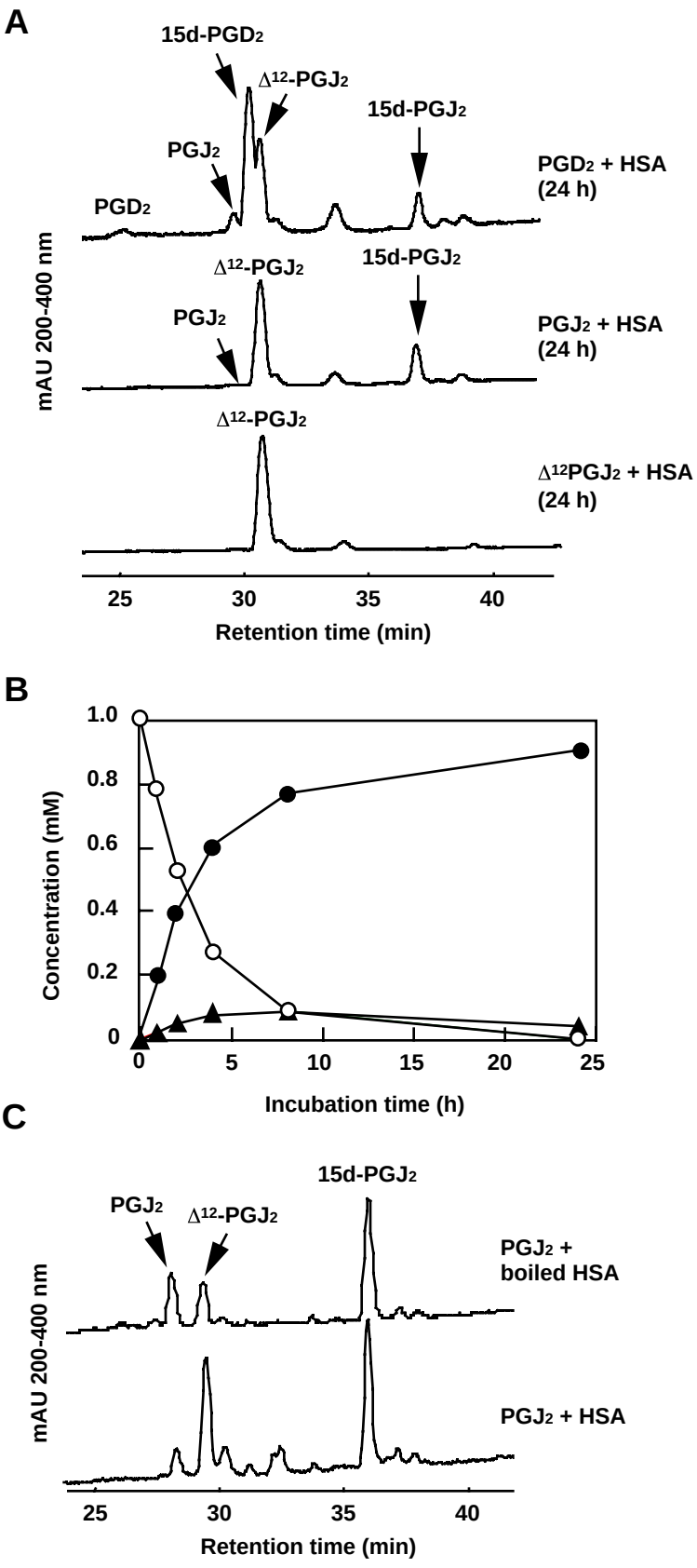

Fig. 8

Shibata et al.

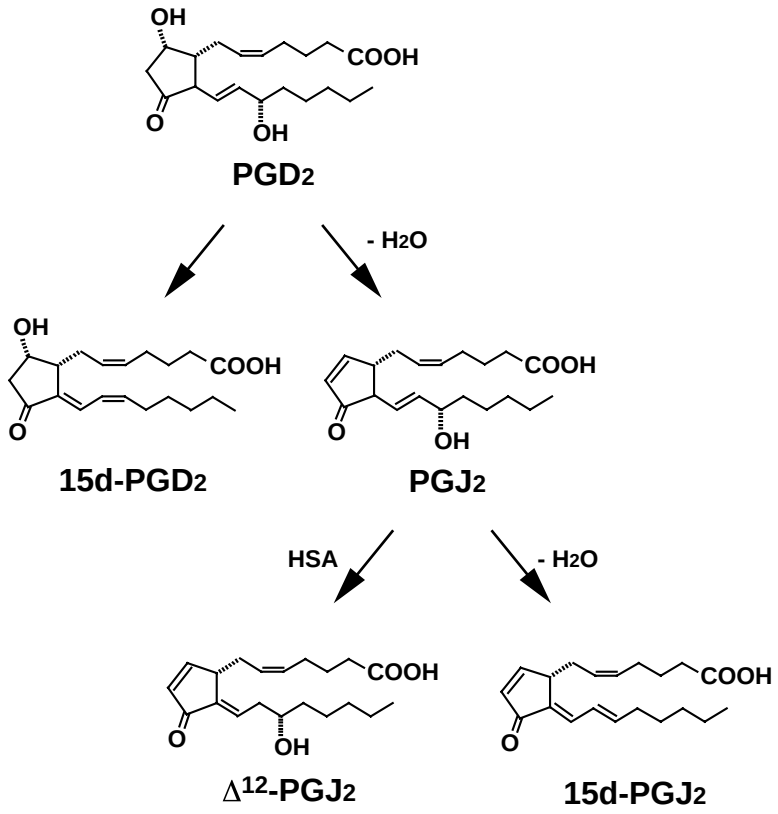

Fig. 9

Shibata et al.

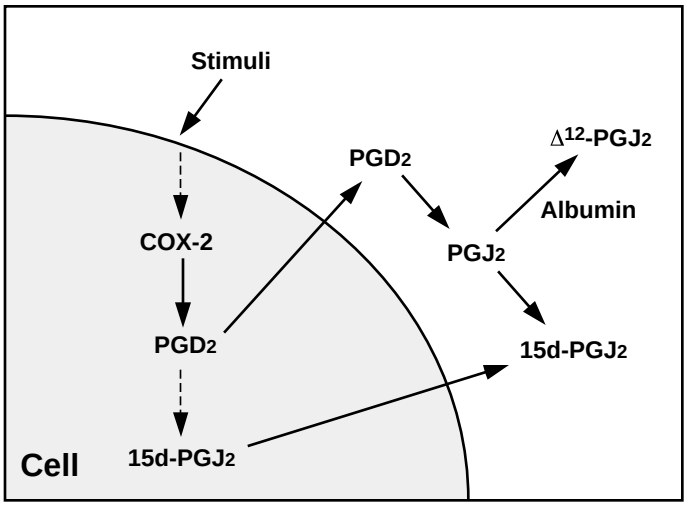

Fig. 10

Shibata et al.

15-Deoxy-delta12,14-prostaglandin J2: A prostaglandin D2 metabolite generated during inflammatory processes

Takahiro Shibata, Mitsuhiro Kondo, Toshihiko Osawa, Noriyuki Shibata, Makio Kobayashi and Koji Uchida

J. Biol. Chem. published online January 10, 2002
